NASA TECHNICAL MEMORANDUM

NASA TM X-1833

NASA TM X-1833

RESULTS OF A FREE-FLIGHT TEST TO DETERMINE THE PERFORMANCE CHARACTERISTICS OF A TOWED, CONICAL DECELERATOR

by J. W. Usry

Langley Research Center

Langley Station, Hampton, Va.

NATIONAL AERONAUTICS AND SPACE ADMINISTRATION • WASHINGTON, D. C. • OCTOBER 1969

RESULTS OF A FREE-FLIGHT TEST TO DETERMINE THE PERFORMANCE CHARACTERISTICS OF A TOWED, CONICAL DECELERATOR

By J. W. Usry
Langley Research Center

SUMMARY

An inflatable fabric decelerator was tested in free flight to determine its drag and stability characteristics. The inflated decelerator approximated an 80^{o} cone with a 48-inch (121.9-cm) base and was towed behind a cone-cylinder-flare payload at a distance of 13.6 feet (4.15 m) from the payload base. The payload had a maximum flare diameter of 18.21 inches (46.25 cm). The decelerator was deployed at an altitude of 112 000 feet (34.14 km) and a velocity of 4560 ft/sec (1390 m/sec). Inflation occurred at a Mach number of 4.31 and a dynamic pressure of 130 lb/ft^2 (6224 N/m^2).

The snatch force after deployment was not more than 500 pounds (2224 N); this low force indicated that the towline assembly design could be simplified for future flights by eliminating the two snubber lines and the nylon sleeve. The shock force due to inflation was 5600 pounds (24.9 kN). After inflation the force in the towline varied between 300 and 1600 pounds (1334 and 7117 N). The oscillatory motion of the decelerator had a high frequency, and the amplitude increased with time. The test was terminated about 1 second after inflation because of a failure at the attachment point of the towline to the decelerator. The results indicated that the decelerator system was unstable and not suitable for use as a supersonic decelerator with the payload used in this experiment under the conditions of the test. A drag coefficient of 0.75 at a Mach number of 4.2 was estimated from the mean value of the force in the towline prior to the failure.

INTRODUCTION

Towed, supersonic decelerator systems are being considered as a means of stabilizing and decelerating spacecraft, research payloads, and expensive booster components. To accomplish these objectives, the decelerator in combination with the primary towing body should be statically and dynamically stable and have a high drag coefficient. In addition the decelerator should be lightweight, easily deployed and inflated, easily constructed, and with minor modifications applicable over a wide range of Mach numbers and dynamic pressures.

Parachutes have been used extensively to decelerate and stabilize airborne bodies in the subsonic regime. Successful operation at supersonic speeds has been demonstrated for large parachutes up to a Mach number of 2.7 at low dynamic pressures and for small parachutes up to a Mach number of 4 at relatively high dynamic pressures. The flow around and through a supersonic parachute however is very complex and frequently leads to instabilities of various types. (See refs. 1 and 2.) Methods that have been used to alleviate instabilities, such as increased porosity, can result in low drag. Nonporous inflatable bodies offer a possible means of providing stable deceleration while maintaining desirably high drag coefficients and of providing these characteristics over a rather wide range of supersonic speeds.

One configuration of a nonporous inflatable decelerator being considered for a supersonic decelerator is the inflatable cone. Wind-tunnel tests reported in reference 3 on an inflatable towed cone and in references 4 and 5 on rigid towed cones indicate favorable drag and stability characteristics.

The purpose of this paper is to present the free-flight test results of an inflatable conical decelerator. The decelerator had an 80° included angle and a base diameter of 48 inches (121.9 cm). The forward end was truncated so that the blunt-nose diameter was 10 inches (25.4 cm). The decelerator was packaged in the flare of the payload, and the payload was accelerated to a velocity of 4560 ft/sec (1390 m/sec) at an altitude of 112 000 feet (34.14 km). At these conditions the decelerator was deployed into the payload wake and towed at a distance of 13.6 feet (4.15 m) from the base of the payload. Approximately 1.5 seconds after deployment the decelerator was inflated at a Mach number of 4.31 and a free-stream dynamic pressure of 130 lb/ft^2 (6224 N/m^2). The test was terminated about 1 second after inflation because of a failure at the attachment point of the towline to the decelerator. Decelerator performance characteristics are discussed by using the basic test measurements.

Motion-picture supplement L-1049 from a camera onboard the payload has been prepared and is available on loan. A request card and description of the film are included at the back of this paper.

SYMBOLS

a_X, a_Y, a_Z linear accelerations along body X-, Y-, and Z-axes, g units

D drag, pounds (newtons)

d payload flare diameter, inches (centimeters)

F	tensiometer force, pounds (newtons)
g	acceleration due to gravity, feet/second^2 (meters/second^2)
h	altitude, feet (kilometers)
l	distance from payload to attachment point of towline to decelerator, inches (centimeters)
M_∞	Mach number
p	roll rate, radians/second
p_i	decelerator internal pressure, pounds/foot^2 (newtons/meter^2)
q	pitch rate, radians/second
q_∞	free-stream dynamic pressure, pounds/foot^2 (newtons/meter^2)
R	radius, inches (centimeters)
r	yaw rate, radians/second
t	time, seconds
V	velocity, feet/second (meters/second)
W	weight, pounds (newtons)
X,Y,Z	body-axis system
x,y	coordinates of decelerator component patterns, inches (centimeters)
α	angle of attack, degrees
β	angle of sideslip, degrees
η	total angle of attack, degrees

TEST CONFIGURATION

A sketch of the flight-test configuration is shown in figure 1. The length from the payload nose to the back of the decelerator was 21 feet (6.4 m). The total weight of the system was 203 pounds (902.9 N). The cone was towed 13.6 feet (4.15 m) downstream of the payload base or about 9 body diameters based on the maximum diameter of the payload flare ($\ell/D = 9$). The ratio of the maximum diameter of the decelerator to the maximum diameter of the payload was 2.64. The payload weight prior to deployment was 203 pounds (902.9 N) and after deployment 179 pounds (796 N). The trailing weight, including the towline assembly and decelerator, was 21 pounds (93.4 N). The center of gravity of the payload was located 29.3 inches (74.4 cm) aft of the nose before deployment and 26.3 inches (66.8 cm) after deployment.

The towline assembly consisted of two snubber lines, the main riser line, and a nylon sleeve. The general arrangement at the payload and decelerator attachment points is shown in figure 1. The purpose of the snubber lines was to absorb the deployment snatch loads. Each line was nylon webbing, 1.00 inch (2.54 cm) wide with a rated strength of 2500 pounds (11.12 kN). The main riser line was one continuous line wrapped twice around the attachment bolts at the payload and decelerator. The line was a high-temperature nylon material, 1.00 inch (2.54 cm) wide with a rated strength of 12 000 pounds (53.4 kN). The nylon sleeve enclosed the snubber lines and main riser line. The ends of the sleeve were constrained at the payload and decelerator attachment points.

Decelerator Description

Photographs of the decelerator from the front and rear are shown in figure 2. Sketches of the decelerator and component patterns and pattern dimensions are shown in figure 3. The decelerator was an inflatable fabric structure symmetrical about the longitudinal axis. The center of gravity was estimated to be 10 inches (25.4 cm) aft of the blunt-nose face.

The inflated decelerator approximated an 80° cone with a 48-inch (121.9-cm) base and was truncated so that the diameter of the blunt nose was about 10 inches (25.4 cm). The length was 32.3 inches (82.0 cm). The fabric in all cloth and webbing was a high-temperature nylon woven material. The fabric was coated with an elastomer for heat protection and to reduce the porosity.

The decelerator was composed of 16 conical compartments with a common theoretical apex. Adjacent cones intersected along two straight lines. At these intersections the fabric of each conical segment was joined to a woven T-section which served as a meridional tension member. Internally, cloth panels (web pattern in fig. 3) were

stitched to the base of the T-sections connecting the outer and inner surfaces of the conical compartments. The ends of each cone were closed by tailored patterns to minimize wrinkling and to eliminate excessive seams. The T-sections, as well as the outer and inner gores of the cones (patterns 5 and 3), were attached to metal rings (patterns 19 and 21). The rings were welded to a toroidal bottle which was used to carry helium for inflating the decelerator.

Payload Description

The payload was a body of revolution 55.98 inches (142.19 cm) long with a hemispherical, blunted 20^{o} half-angle conical nose, a cylindrical centerbody, and a 10^{o} half-angle flare with four fins. A sketch of the payload with dimensions and pertinent details is shown in figure 4. The four principal structural components were the blunted cone-cylinder forebody, an instrument support deck, the cylindrical centerbody, and the flared afterbody.

The forebody was 18.50 inches (46.99 cm) long with a 3.76-inch-radius (9.55-cm) hemispherical nose on a 20^{o} half-angle cone-cylinder section. The forebody enclosed the instrument support deck, and both were electrically insulated from the rest of the payload by the telemeter antenna ring. The centerbody was 18.50 inches (46.99 cm) long with a 12-inch (30.48-cm) diameter. The aft end of the centerbody was closed by a cover plate. The plate was machined and threaded on the aft surface to accept the separation bolt which attached the flare to the centerbody. The flare was 18.63 inches (47.32 cm) long and had a maximum diameter of 18.21 inches (46.25 cm). A cylindrical sleeve, which was part of a bulkhead in the forward end of the flare, mated with the centerbody cover plate and enclosed the explosive bolt. The inside diameter of the aft end of the sleeve was threaded to accept a tensiometer to which the decelerator towline was attached. The fins on the flare had a leading-edge sweep angle of 70^{o} and a leading-edge radius of 0.1 inch (0.254 cm). The cross section of the fin was wedge-shaped with a 14^{o} half-angle in a plane normal to the body center line. The aft end of the flare housed the packaged decelerator during the boost phase of the mission.

INSTRUMENTATION

A telemeter transmitted ten continuous channels of information. These transmissions included two longitudinal accelerations; two lateral accelerations; pitch, yaw, and roll rates; a tensiometer measurement of the tension in the towline; two differential pressure measurements on the payload nose; the decelerator internal pressure; and one channel to correlate photographic data with telemetered data. The pressure data were commutated and transmitted on one channel. Pressure measurements were recorded at intervals of approximately 0.1 second.

A motion-picture camera was located in the payload centerbody as shown in figure 4. The lens axis was parallel to the payload center line, faced rearward, and was located 3.08 inches (7.82 cm) from the center line. The total view angle was 60°, 9° being obstructed by the payload flare. The field of view in a plane at the decelerator was about 3 decelerator body diameters.

The following table lists the measurements, instrument ranges, and the expected accuracy of each instrument:

Measurement	Range	Accuracy, percent total range
Linear acceleration, a_X, high . . .	-15g to 68g	±2
Linear acceleration, a_X, low	-5g to 1g	±2
Linear acceleration, a_Y, a_Z . . .	±5g	±2
Roll rate, p	±15 rad/sec	±2
Pitch rate, q	±10 rad/sec	±2
Yaw rate, r	±10 rad/sec	±2
Differential pressure	±2 psi (±13.79 kN/m^2)	±4
Decelerator internal pressure . . .	0 to 10 psi (0 to 68.95 kN/m^2)	±4
Tensiometer force	0 to 9000 lb (0 to 40.03 kN)	±3

The orientation of the body-axis system for the measured and computed quantities is shown in figure 5. Linear accelerations and tensiometer force were measured positive in the positive directions of the X-, Y-, and Z-axes.

RESULTS AND DISCUSSION

Test Environment

The test environment was achieved with the use of a three-stage rocket-boosted launch vehicle. The mission profile is shown in figure 6. The payload after separating from the third-stage booster coasted on an ascending trajectory for approximately 10 seconds before decelerator deployment was started. Deployment was accomplished by firing a 2-pound (8.9-N) weight rearward with a line attached to the weight and the decelerator. Approximately 1.5 seconds after deployment the decelerator inflated at h = 118 700 feet (36.2 km) and V = 4445 ft/sec (1355 m/sec) or M_∞ = 4.31 and q_∞ = 130 lb/ft^2 (6224 N/m^2).

Variations of atmospheric pressure, density, and speed of sound with altitude are presented in figure 7. These conditions were measured approximately 1 hour after the flight. The measured quantities were compared with the U.S. Standard Atmosphere Supplements, 1966 (ref. 6) and were estimated to be accurate within ±3 percent.

Altitude, horizontal-range, and velocity data were calculated from the best available radar track of the payload. Mach number and dynamic pressure were calculated from the radar data and the measured atmospheric data. Altitude and velocity time histories are shown in figure 8 and Mach number and dynamic pressure in figure 9. The velocity data were estimated to be accurate within ±100 ft/sec (30.5 m/sec).

Data Presentation

Histories of the tensiometer force, longitudinal acceleration, and deceleration internal pressure are shown in figure 10. Photographs from the motion-picture camera are presented in figure 11, and times at which selected photographs were made are indicated in figure 10. Figure 12 shows histories of the pitch, yaw, and roll rates of the payload; accelerations along the Y- and Z-axes; and estimated total angles of attack. The angles were estimated from measured differential pressures on the payload nose. The histories extend from $t = 60$ seconds, 0.1 second before deployment, to $t = 63$ seconds, 0.5 second after a failure occurred at the attachment point of the towline to the decelerator; this failure ended the experiment.

Decelerator Performance

Deployment and inflation.- Deployment was started when the drogue gun fired and the packaged decelerator was extracted from the flare into the payload wake. The gun fired at $t = 60.1$ seconds as indicated in figure 10. The first snubber line was at full extension (not stretched) 0.46 second after the gun fired. A pull-pin pyrotechnic cutter should have cut the line 0.25 second after the load exceeded 10 pounds (44.5 N) and allowed the packaged decelerator to move rearward to full extension of the second snubber line. The second line should have experienced a similar sequence of events.

The purpose of the two lines was to allow the packaged decelerator to move rearward in steps as the lines were cut; thereby the relative velocity between the two bodies at full extension of the main towline would be minimized. The data shown in figure 10 indicate that the deployment loads were considerably less than anticipated. The snatch force of 500 pounds (2224 N) was about one-third the expected value. Also the loads after the initial snatch force and prior to inflation were less than 300 pounds (1334 N). These data and the results of reference 7 do indicate, however, that the towline design for this test condition can be simplified by eliminating the two snubber lines and the nylon sleeve.

Inflation was started at $t = 61.5$ seconds as shown in figure 10. The maximum shock load was 5600 pounds (24.9 kN). After the initial shock load, the force measurement was zero from $t = 61.61$ seconds to $t = 61.65$ seconds. If the snubber lines, one or both, had not been cut prior to inflation as planned, the lines would have been broken because of the inflation shock load. The absence of a load during this time could possibly

be the time required for the decelerator to move rearward to full stretch of the main towline after the snubber lines were broken because of the inflation shock load. Another possibility is that the decelerator rebounded far enough forward to cause the line to become slack. The photographic data in figure 11 appear to support the first possibility. Photograph 4 was made just prior to the time that the shock load occurred but after inflation had started. Photograph 5 was made during the application of the shock load, and photographs 6 and 7 were made when the tensiometer force was zero. All the photographs show the view partially obscured by the towline cover (nylon sleeve); this obstruction would be expected if the main towline were not fully extended. Photographs after photograph 7 show the expected view with the towline fully extended. The times indicated in figure 10, at which the photographs were made, were matched with the times indicated for the acceleration and tensiometer measurement and were estimated to be within ±0.03 second.

Stability.- After inflation the payload-decelerator system did not recover to a stable condition before the decelerator was lost at $t = 62.5$ seconds. The data presented in figure 10 indicate that the decelerator was bouncing or flagging on the towline. The photographic data in figure 11 show that the initial decelerator oscillations were small but increased with time. Photographs made just before the decelerator was lost show its longitudinal axis nearly normal to the flow.

The payload lateral accelerations and pitch and yaw body rates were small before and after inflation as shown in figure 12. Accelerations were less than 0.5g and pitch and yaw rates less than 2 rad/sec. The payload roll rates shown in figure 12 were induced by the last rocket motor stage and were not significantly affected by the decelerator. Estimated flow incidence angles of the payload increased to a maximum of 10° before the decelerator was lost. Basically, the results of figures 10, 11, and 12 show that the decelerator system was unstable and not suitable as a supersonic decelerator in combination with the payload used in this experiment under the conditions of the test.

The reasons for the instability are not apparent from the data obtained. It is suggested, however, that the instability was associated with the decelerator and not with the payload or towline. Reference 7 presents the results of a free-flight test of a ballute decelerator in which the same payload and towline assembly were used. The ballute was deployed at a Mach number of 4.2 and dynamic pressure of 163 lb/ft^2 (7.8 kN/m^2) and was stable. The front surface of the ballute approximated an 80° cone, and the rear surface was a spherical segment. The ballute had an equatorial diameter of 40 inches (101.6 cm) and a 10-percent burble fence.

Results of wind-tunnel tests on towed 80° cones are presented in references 3, 4, and 5. None of these models exhibited the dynamic instability observed in the present flight. As in the test reported herein, measurements of the stability of these models were made by observing the performance by using high-speed photography. An inflatable model

was used for the tests in reference 3, and rigid models were used for the tests in references 4 and 5. The inflatable model was towed behind a cone-cylinder payload, and the rigid models were towed behind a cone-cylinder-flare payload. The ratio of the decelerator diameter to the payload diameter was 2.92 for the inflatable models and 0.89 for the rigid models. The distance that the decelerators were towed downstream of the payload base was varied for all tests.

The inflatable model and the rigid model of reference 4 had sharp conical nose tips whereas the model of reference 5 had a blunt nose with a diameter which was about 10 percent of the base diameter. The rigid models had sharp shoulders at the cone base, and the inflatable model had rounded shoulders with a radius of about 7 percent of the base diameter. The model reported herein had a blunt nose with a diameter of about 20 percent of the base diameter and rounded shoulders at the decelerator base with a maximum radius which was 10 percent of the base diameter.

Drag.- The tensiometer force shown in figure 10 varied between 300 and 1600 pounds (1334 and 7117 N) after inflation. By assuming that the mean value just after inflation is the steady-state value, the drag of the decelerator can be approximated by

$$D_2 = F\left(\frac{W_1 + W_2}{W_1}\right) + D_1\left(\frac{W_2}{W_1}\right)$$

where the subscripts 1 and 2 refer to the payload and decelerator, respectively. The payload drag was calculated by using the best estimates of drag coefficient from reference 8, measured longitudinal acceleration data, and the free-stream velocity and density. A drag coefficient of 0.75 was estimated for a Mach number of 4.2, a dynamic pressure of 120 lb/ft^2 (5746 N/m^2), and a reference area of 4π feet^2 (1.17 m^2). Interpolation of the results of references 3, 4, and 5 indicated that the drag coefficient varied from 0.69 to 0.86 at $M_\infty = 4.2$.

CONCLUDING REMARKS

The results of a free-flight test of an inflatable conical decelerator were determined. The decelerator was deployed at an altitude of 112 000 feet (34.14 km) at a free-stream velocity of 4560 ft/sec (1390 m/sec). After deployment the decelerator was inflated at a Mach number of 4.31 and a dynamic pressure based on free-stream conditions of 130 lb/ft^2 (6224 N/m^2). The snatch force after deployment was not more than 500 pounds (2224 N); thus, the towline assembly design can be simplified for future flights by eliminating the two snubber lines and the nylon sleeve. The shock force due to inflation was 5600 pounds (24.9 kN). After inflation the force in the towline varied between 300 and 1600 pounds (1334 to 7117 N). The oscillatory motion of the decelerator had a high

frequency, and the amplitude increased with time. The test was terminated about 1 second after inflation because of a failure at the attachment point of the towline to the decelerator. The results indicate that the decelerator system was unstable and not suitable for use as a supersonic decelerator with the payload used in this experiment under the conditions of the test. A drag coefficient of 0.75 at a Mach number of 4.2 was estimated from the mean value of the force in the towline prior to the failure.

Langley Research Center,
National Aeronautics and Space Administration,
Langley Station, Hampton, Va., July 22, 1969,
124-07-03-05-23.

REFERENCES

1. Maynard, Julian D.: Aerodynamics of Decelerators at Supersonic Speeds. Proceedings of the Recovery of Space Vehicles Symposium, Inst. Aeronaut. Sci., Aug.-Sept. 1960, pp. 48-54.

2. Maynard, Julian D.: Aerodynamic Characteristics of Parachutes at Mach Numbers From 1.6 to 3. NASA TN D-752, 1961.

3. McShera, John T., Jr.: Aerodynamic Drag and Stability Characteristics of Towed Inflatable Decelerators at Supersonic Speeds. NASA TN D-1601, 1963.

4. Charczenko, Nickolai; and McShera, John T.: Aerodynamic Characteristics of Towed Cones Used as Decelerators at Mach Numbers From 1.57 to 4.65. NASA TN D-994, 1961.

5. Charczenko, Nickolai: Aerodynamic Characteristics of Towed Spheres, Conical Rings, and Cones Used as Decelerators at Mach Numbers From 1.57 to 4.65. NASA TN D-1789, 1963.

6. Anon.: U.S. Standard Atmosphere Supplements, 1966. Environ. Sci. Serv. Admin., NASA, and U.S. Air Force.

7. Usry, J. W.: Performance of a Towed, 48-Inch-Diameter (121.92-cm) Ballute Decelerator Tested in Free Flight at Mach Numbers 4.2 to 0.4. NASA TN D-4943, 1969.

8. Anon.: Handbook of Supersonic Aerodynamics. Section 8 – Bodies of Revolution. NAVWEPS Rep. 1488 (Vol. 3), U.S. Govt. Printing Office, Oct. 1961.

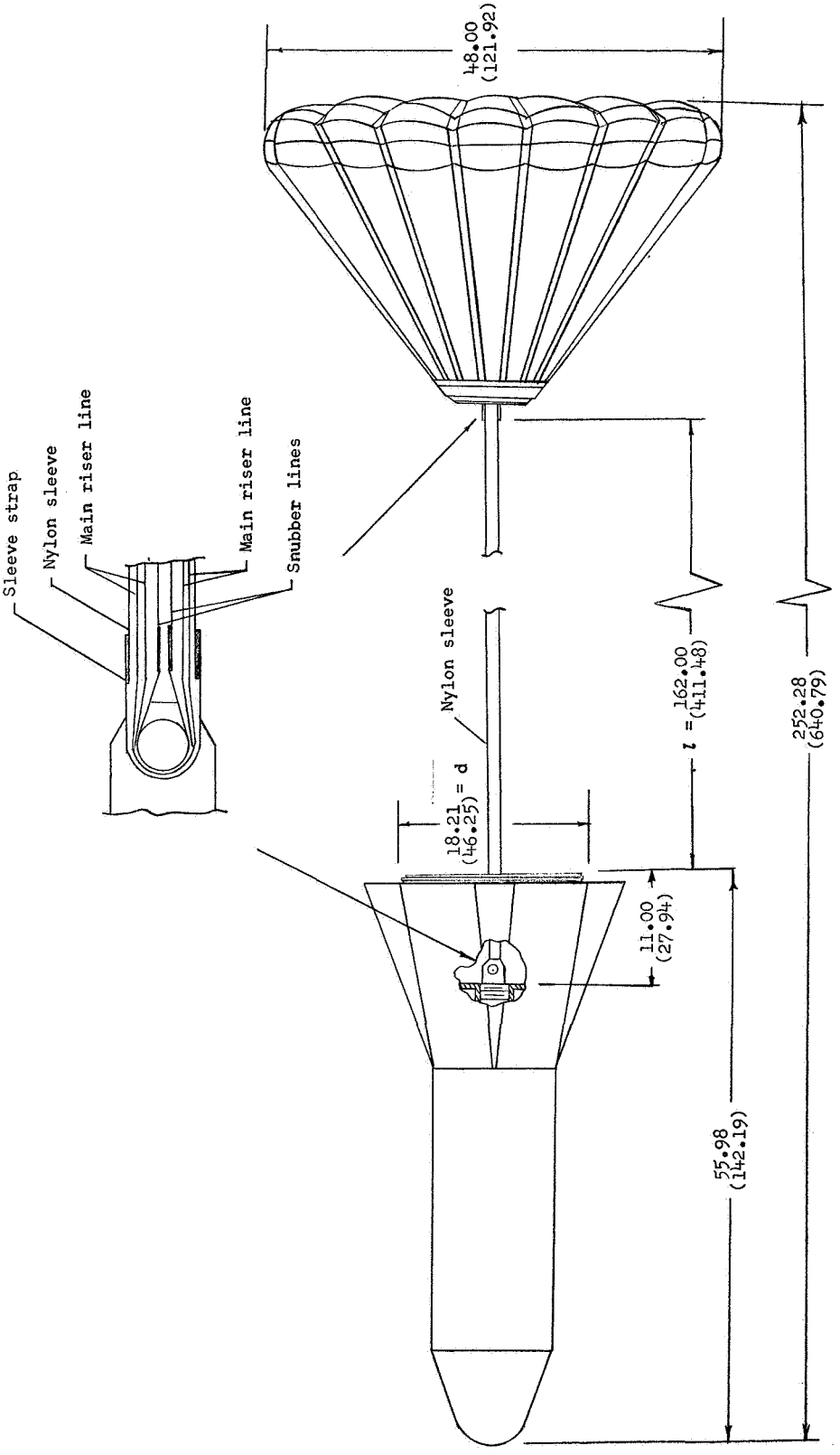

Figure 1.- Flight-test configuration. Dimensions are in inches (centimeters).

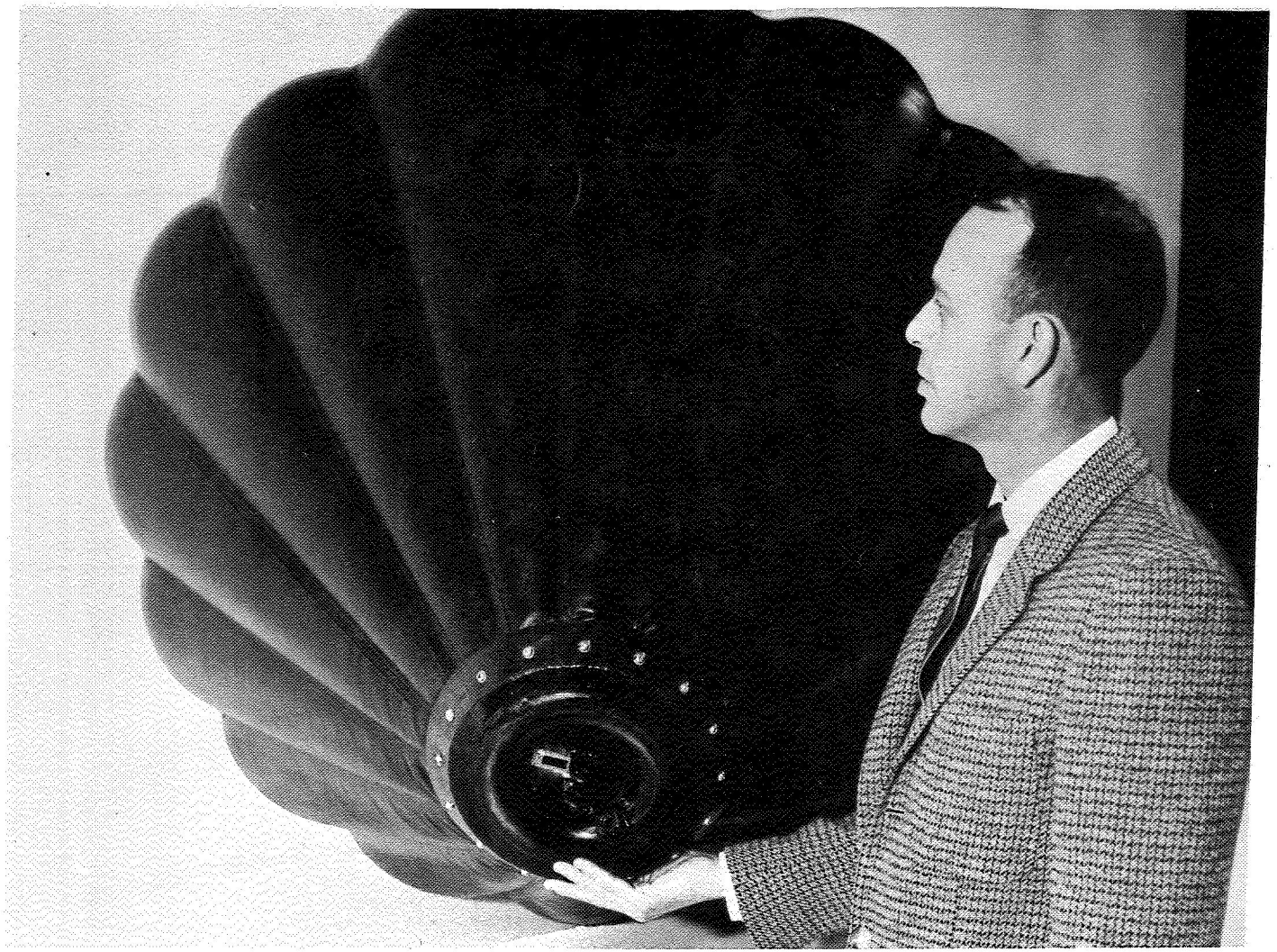

(a) Front.

L-69-5259

Figure 2.- Photographs of decelerator.

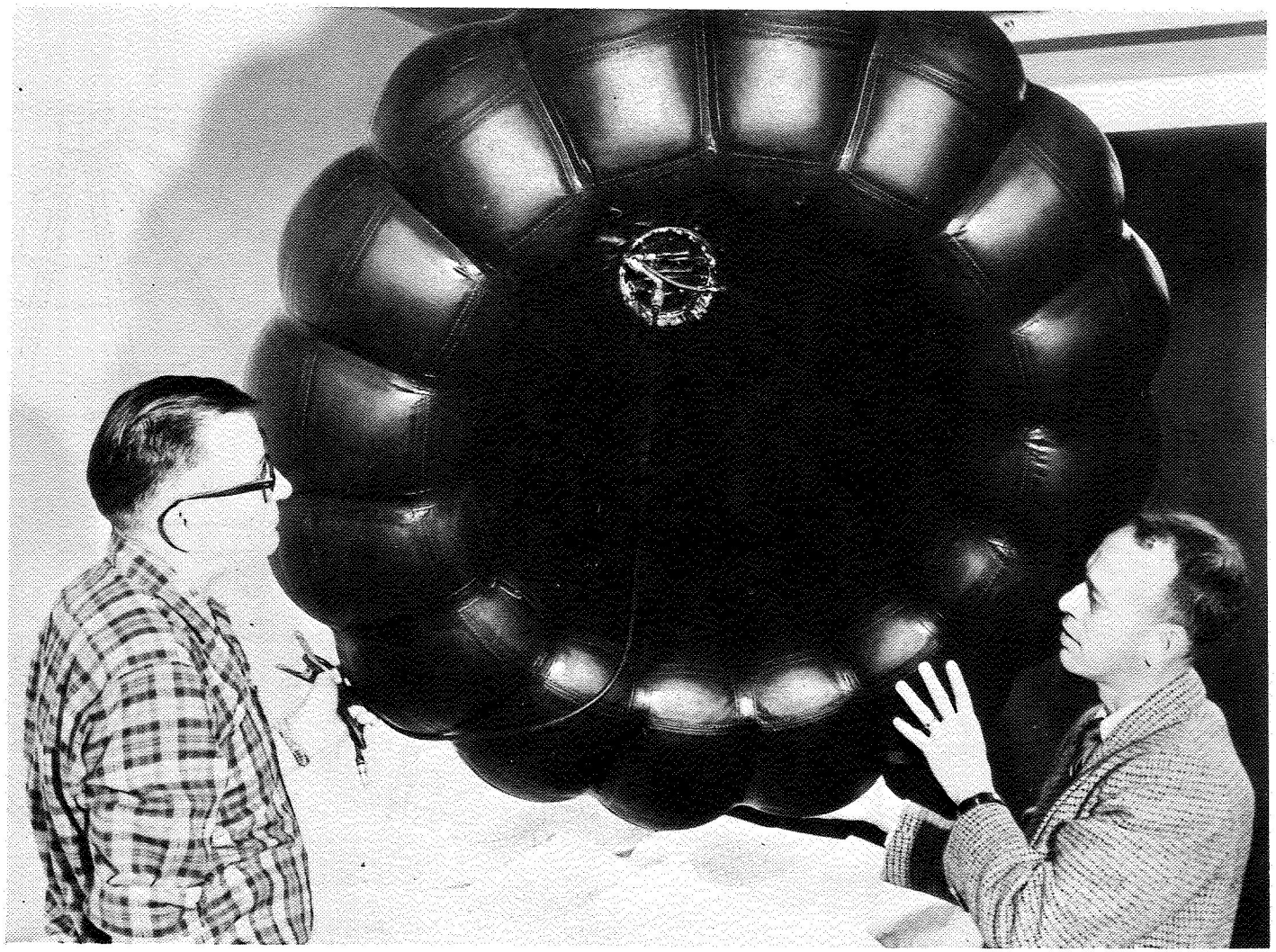

(b) Rear.

L-69-5260

Figure 2.- Concluded.

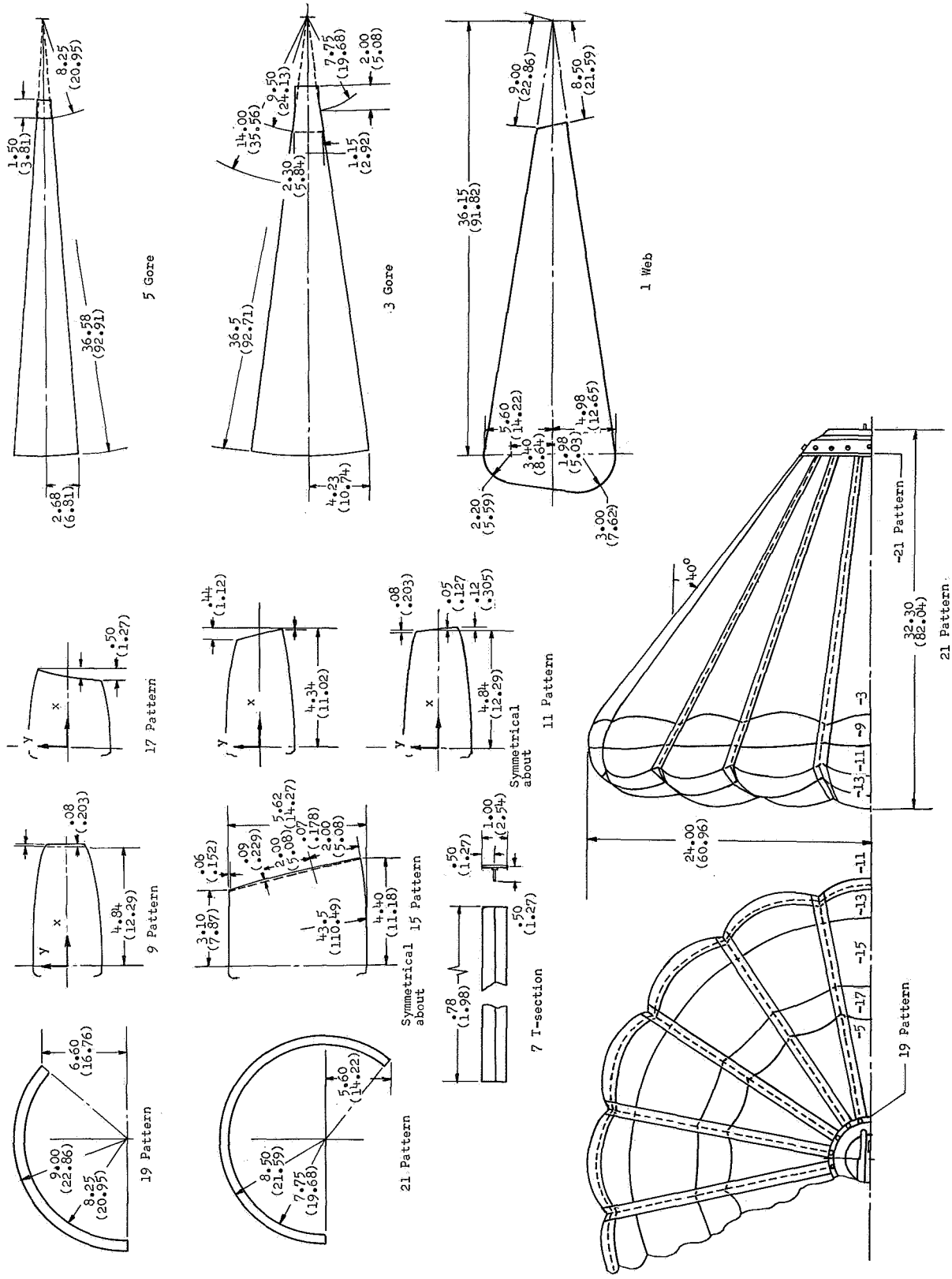

Figure 3.- Sketch of decelerator and component patterns. Dimensions are in inches (centimeters).

PATTERN DIMENSIONS

Inches

9 Pattern		11 Pattern		13 Pattern		17 Pattern	
x	y	x	y	x	y	x	y
0.00	1.41	0.00	1.41	0.00	1.41	0.00	1.68
1.00	1.38	1.00	1.38	1.00	1.38	1.00	1.64
2.00	1.32	2.00	1.32	2.00	1.32	2.00	1.53
3.00	1.22	3.00	1.22	3.00	1.21	2.50	1.44
4.00	1.07	4.00	1.07	4.00	1.04	3.00	1.32
4.50	.97	4.50	.97	4.84	.83	---	---
4.84	.89	4.84	.89	---	---	---	---
4.92	.00	4.89	.00	---	---	---	---

Centimeters

9 Pattern		11 Pattern		13 Pattern		17 Pattern	
x	y	x	y	x	y	x	y
0.00	3.58	0.00	3.58	0.00	3.58	0.00	4.27
2.54	3.51	2.54	3.51	2.54	3.51	2.54	4.17
5.08	3.35	5.08	3.35	5.08	3.35	5.08	3.89
7.62	3.10	7.62	3.10	7.62	3.07	6.35	3.66
10.16	2.72	10.16	2.72	10.16	2.64	7.62	3.35
11.23	2.46	11.23	2.46	12.29	2.11	---	---
12.29	2.26	12.29	2.26	----	---	---	---
12.49	.00	12.42	.00	----	---	---	---

Figure 3.- Concluded.

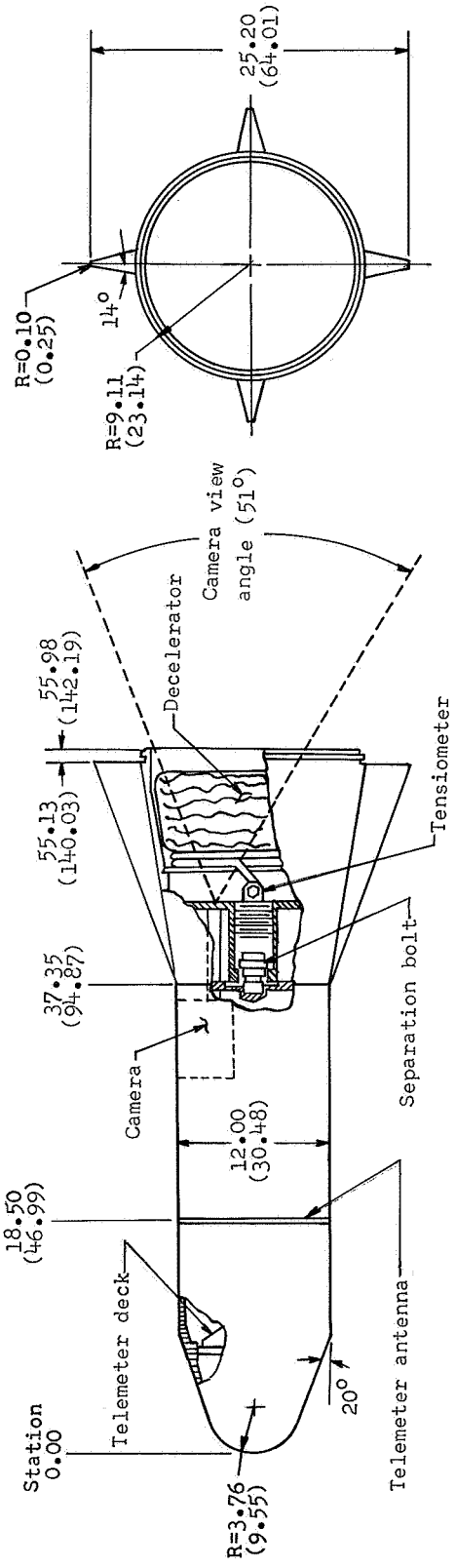

Figure 4.- Sketch of payload. Dimensions are in inches (centimeters) and degrees. (Sketch is not to scale.)

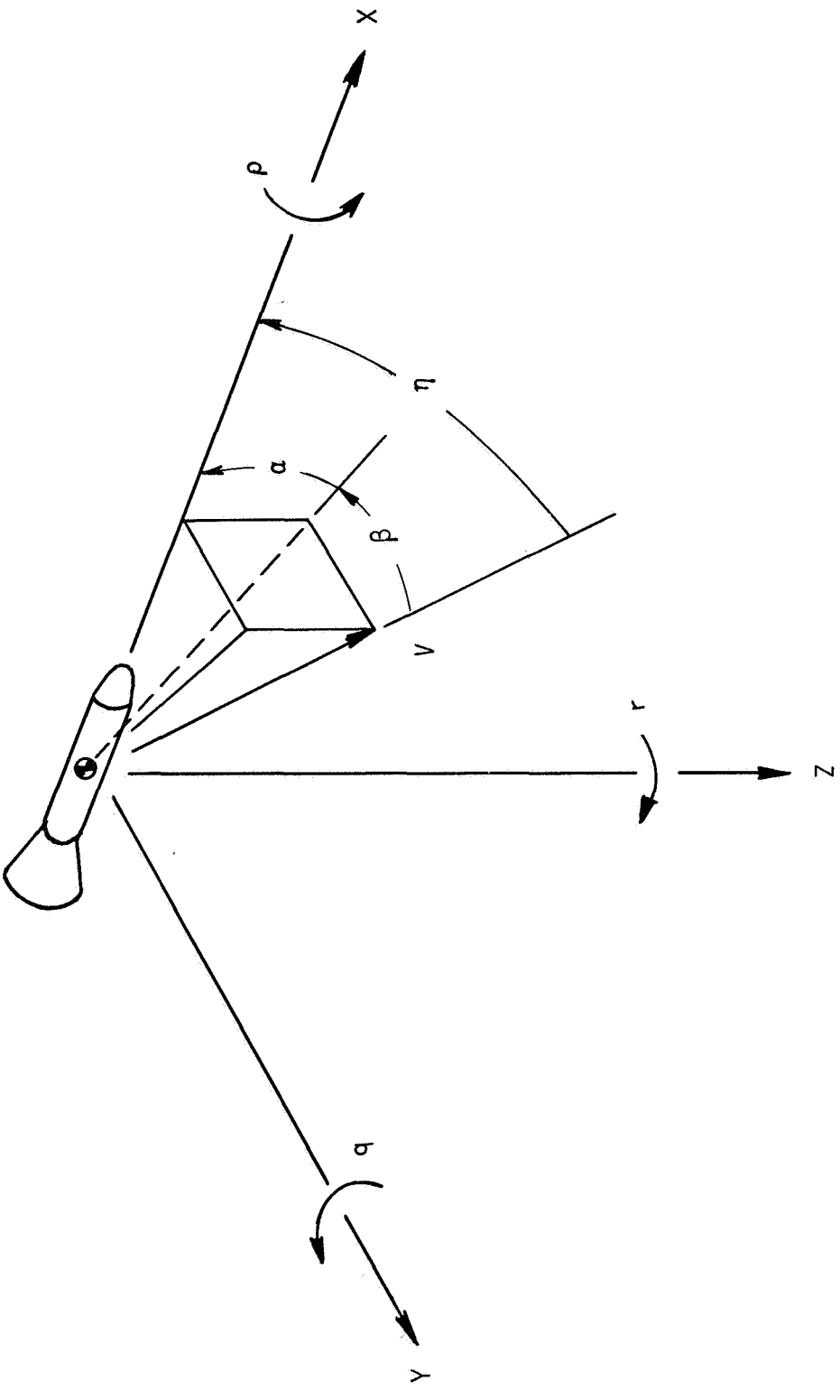

Figure 5.- Orientation of body-axis system.

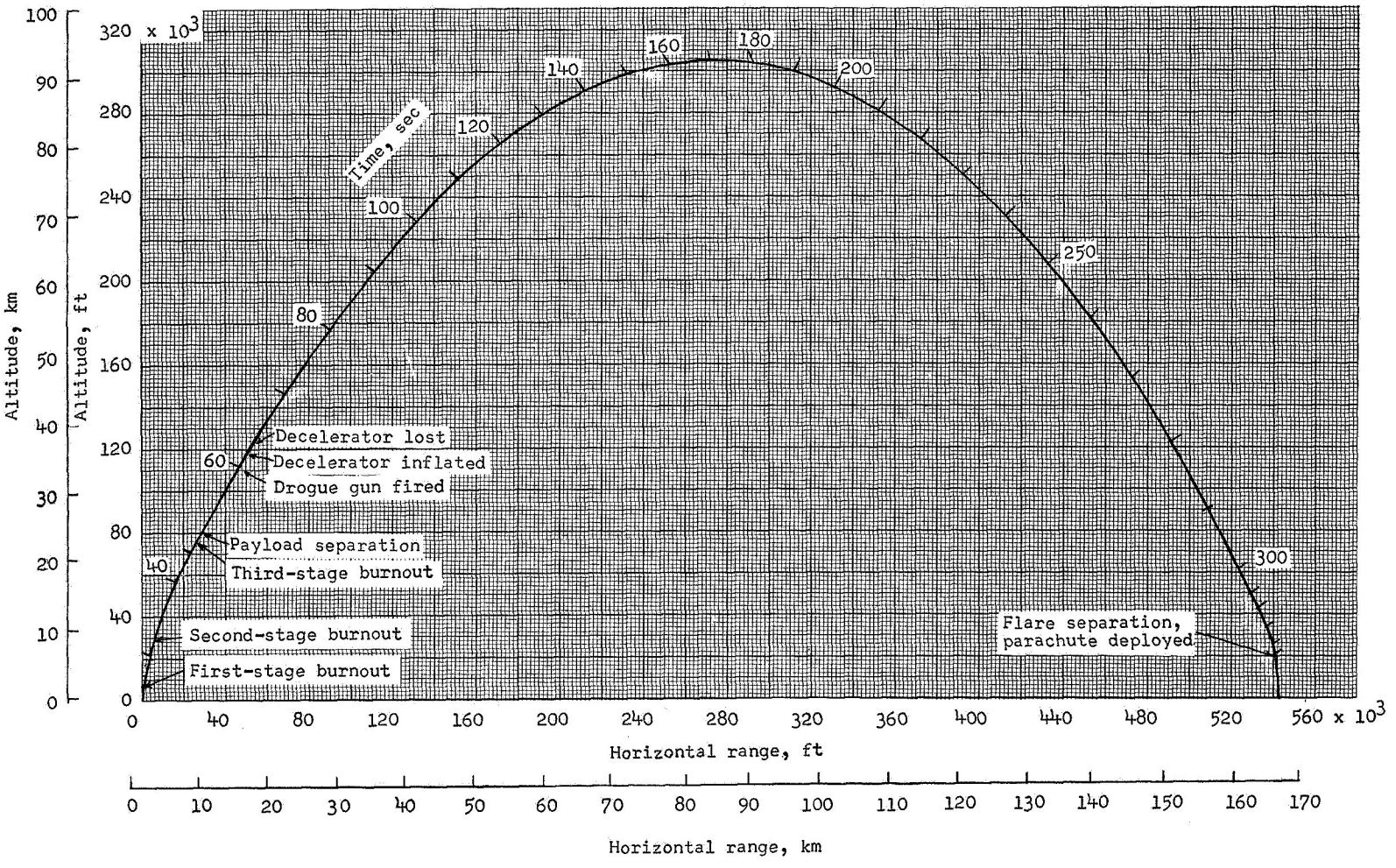

Figure 6.- Variation of altitude with horizontal range.

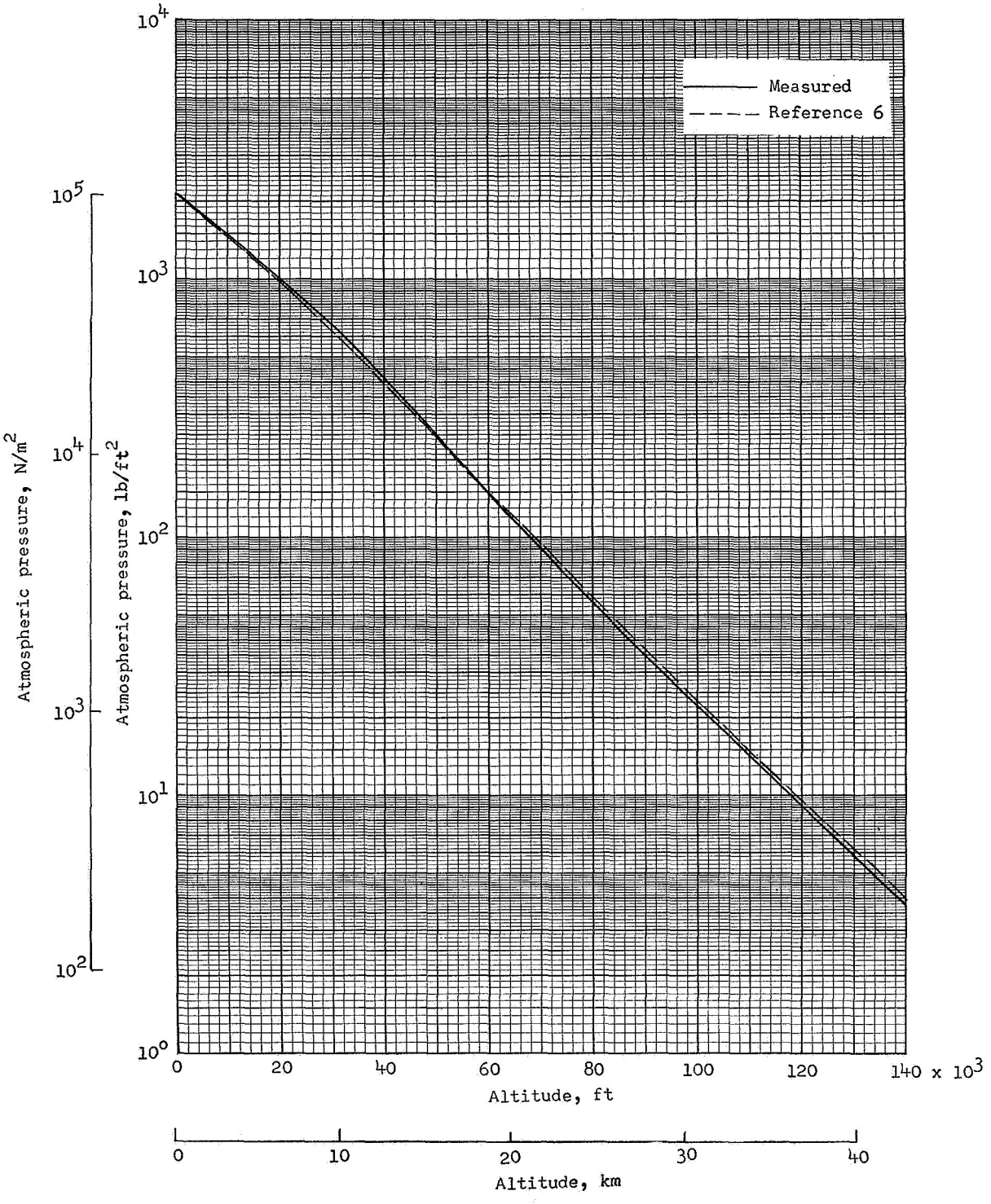

(a) Pressure.

Figure 7. - Variation of pressure, density, and speed of sound with altitude.

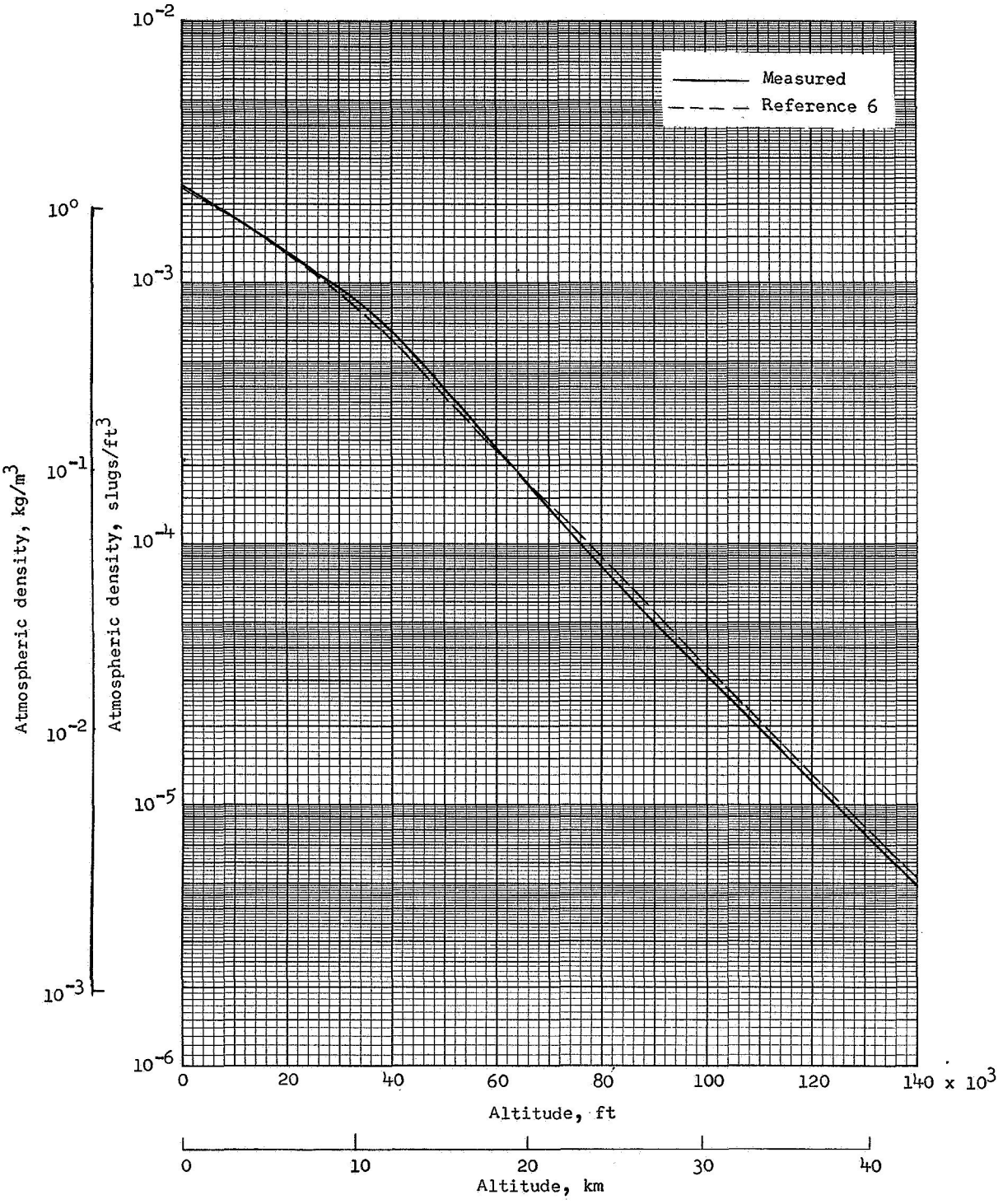

(b) Density.

Figure 7.- Continued.

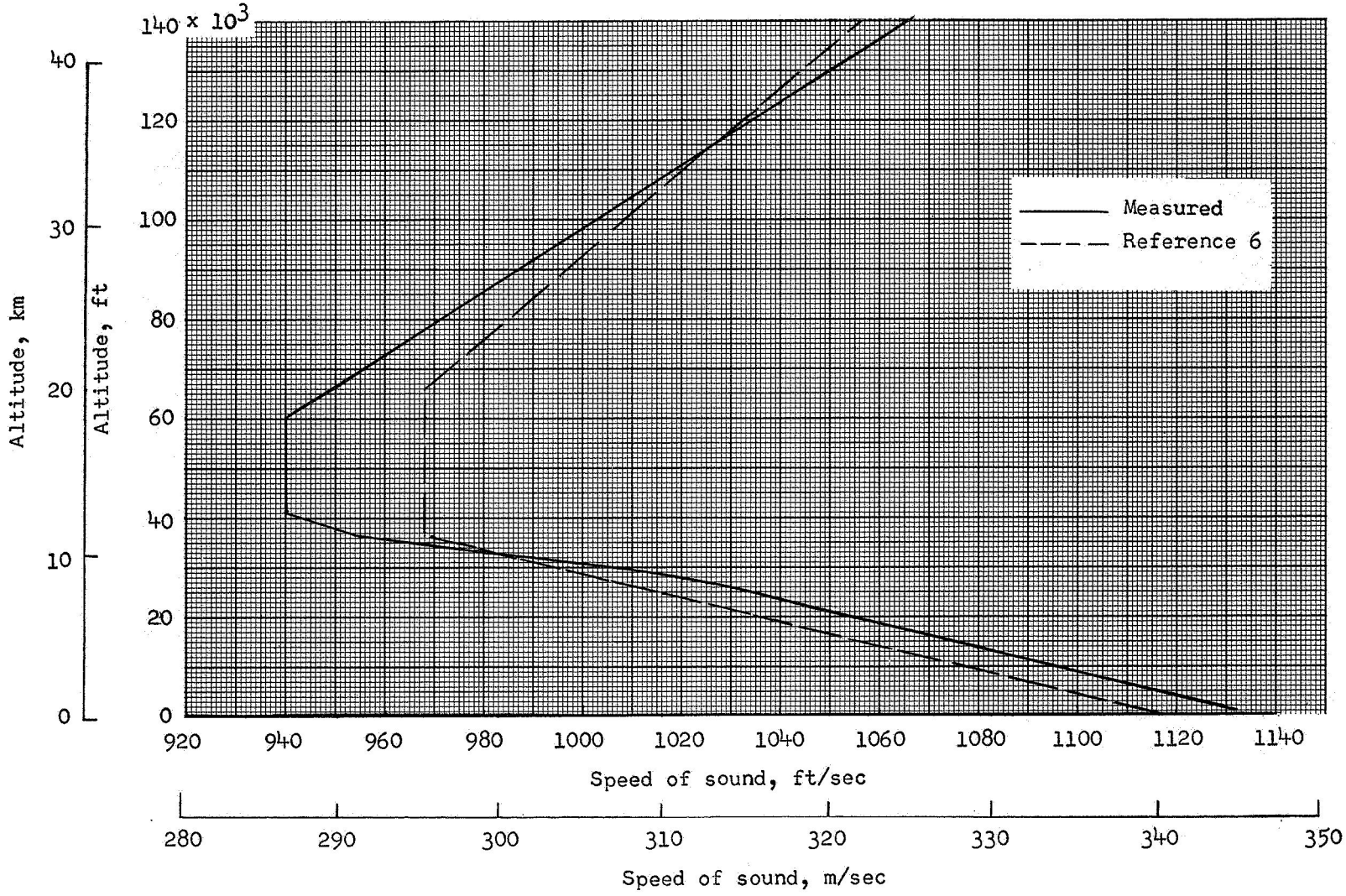

(c) Speed of sound.

Figure 7.- Concluded.

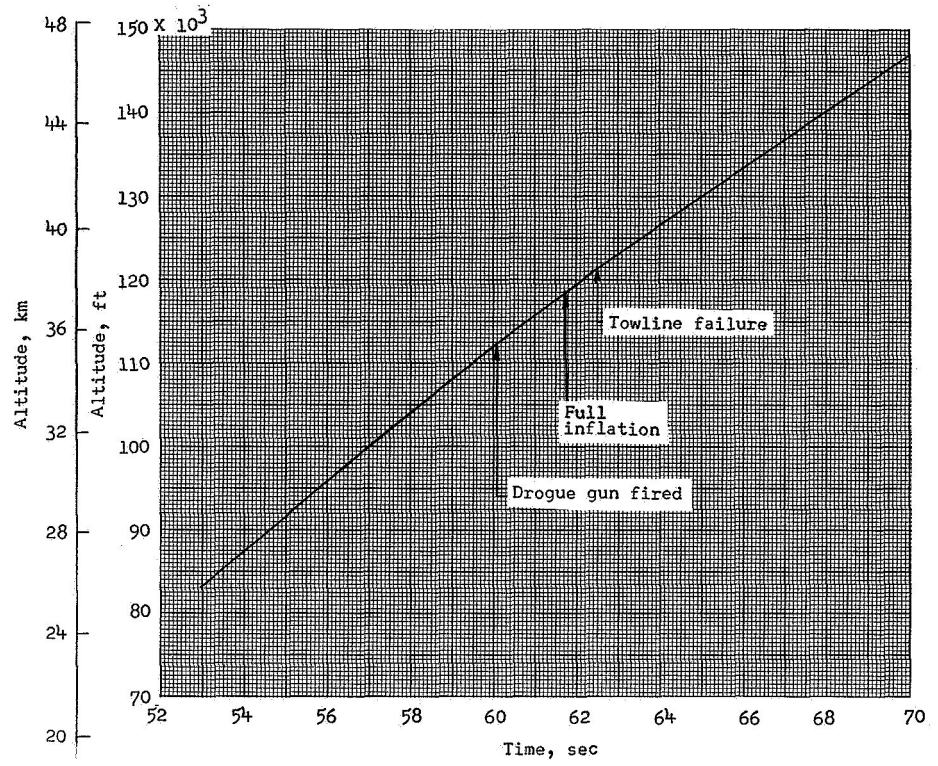

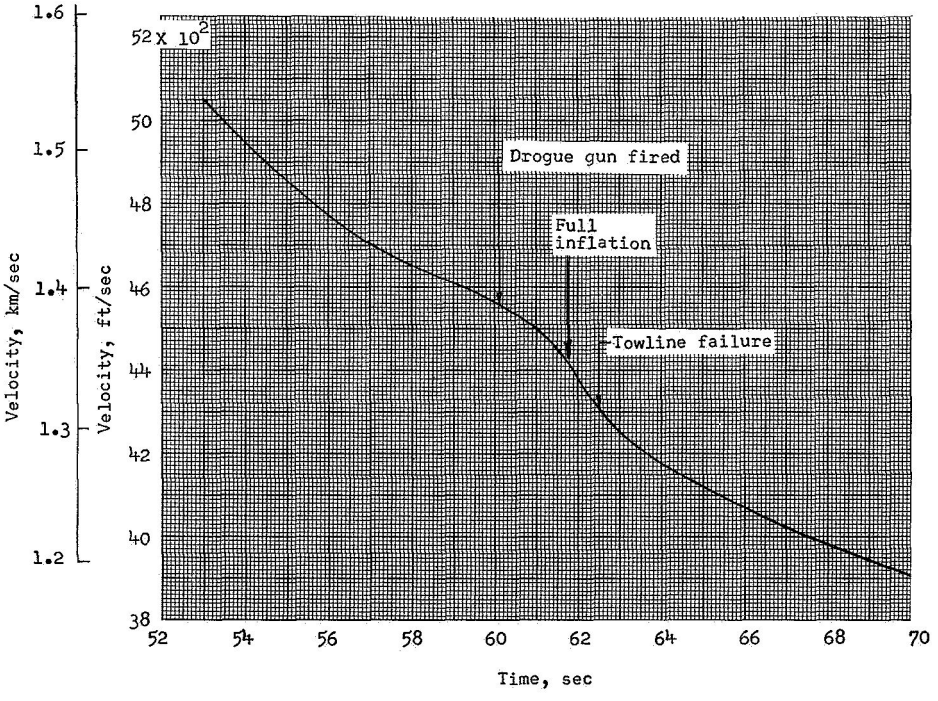

Figure 8.- Variation of altitude and velocity with time.

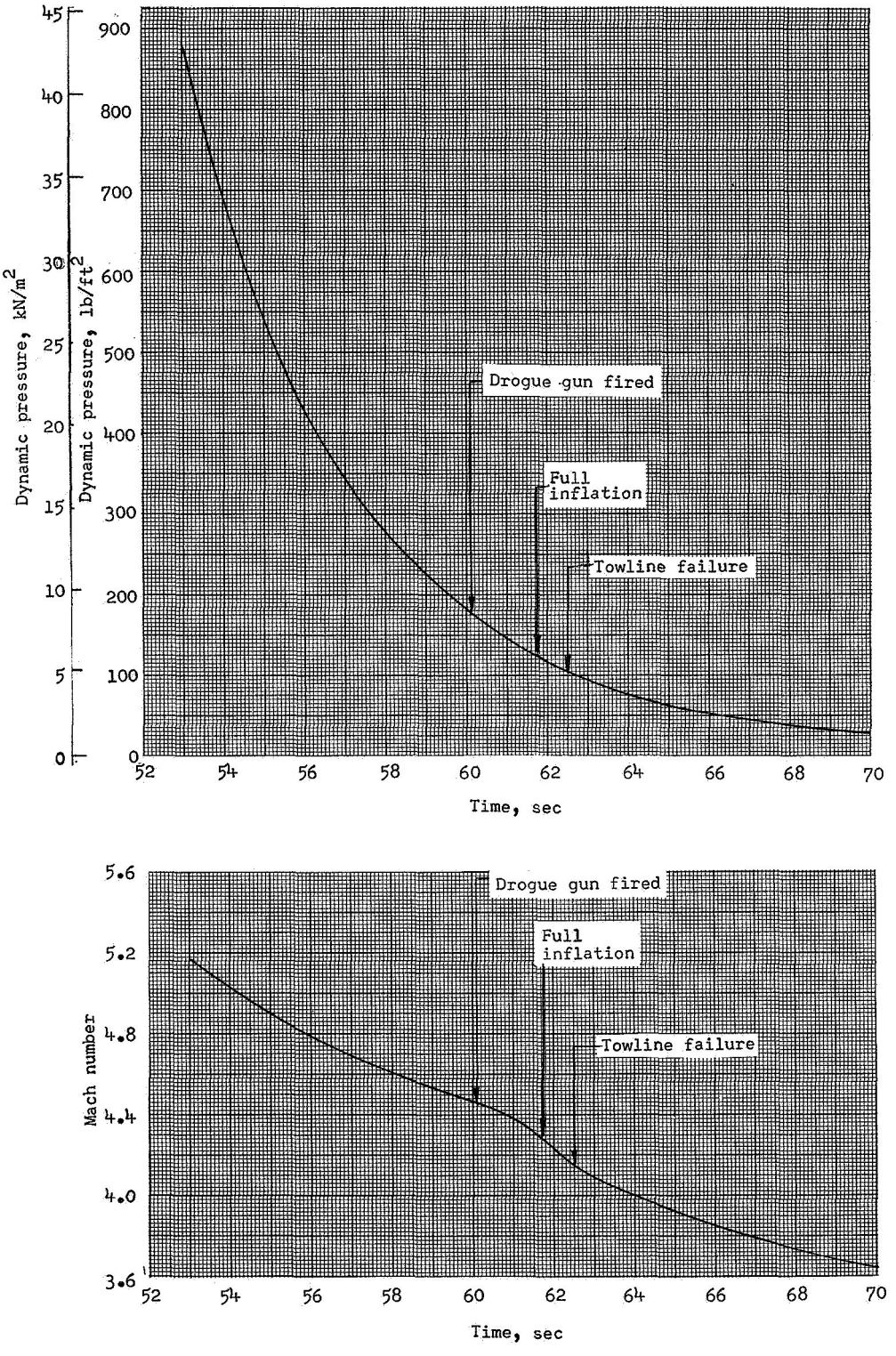

Figure 9.- Variation of dynamic pressure and Mach number with time.

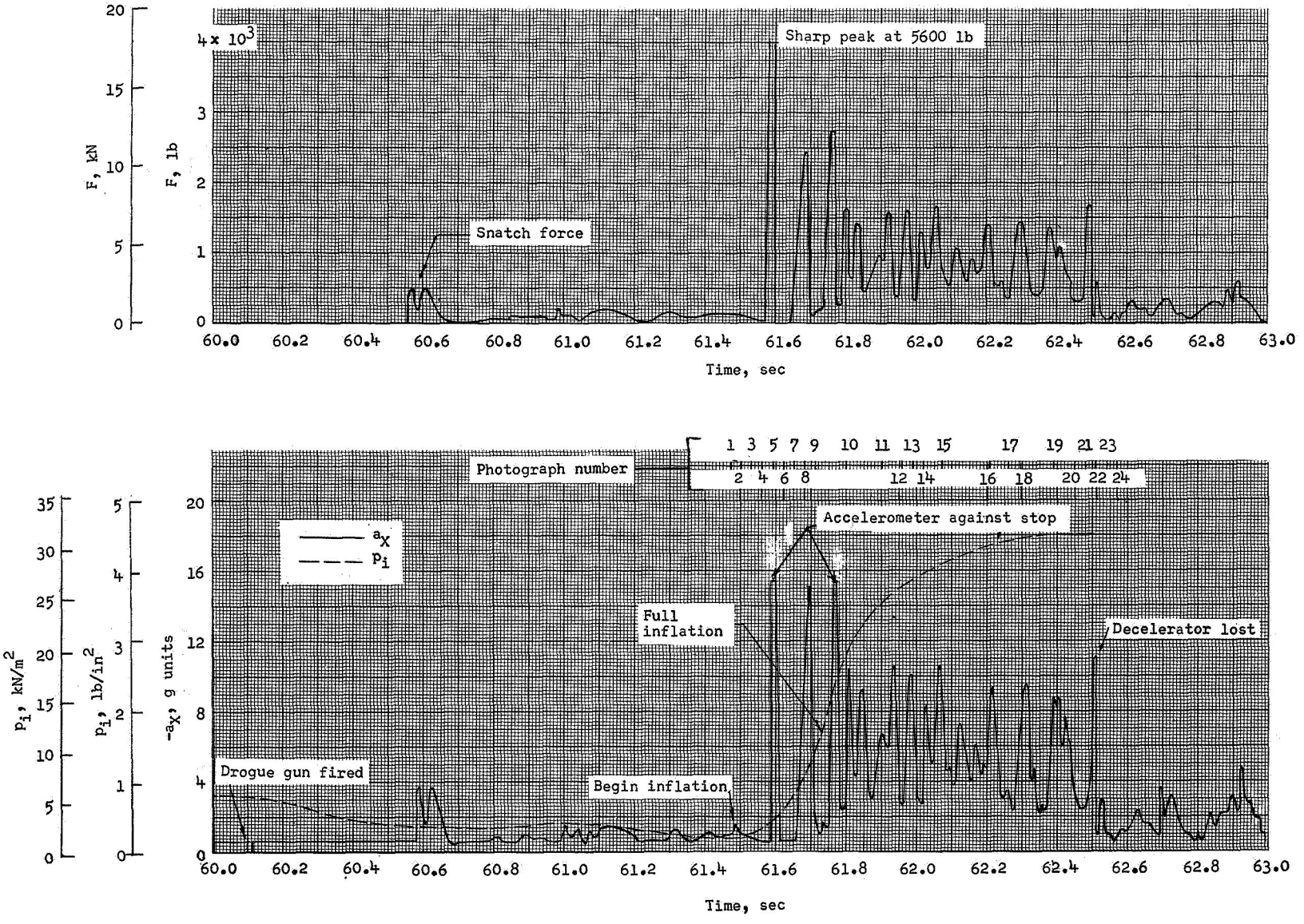

Figure 10.- Variation of tensiometer force, longitudinal acceleration, and decelerator internal pressure with time.

1

t = 61.47

2

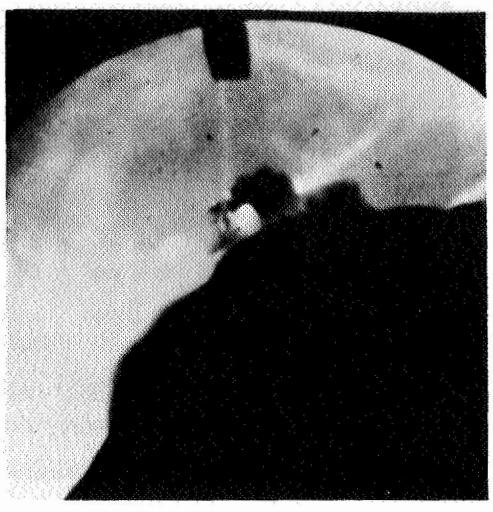

t = 61.50

3

t = 61.53

4

t = 61.56

L-69-5261

Figure 11.- Photographs of decelerator from onboard camera. (Numbers at the left of photographs indicate sequence.)

5

t = 61.59

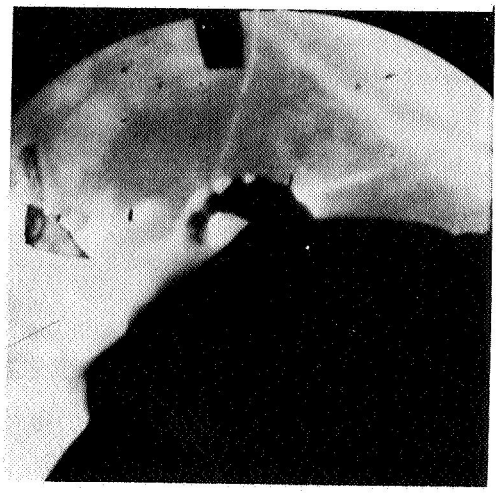

6

t = 61.62

7

t = 61.65

8

t = 61.68

Figure 11.- Continued.

L-69-5262

9

t = 61.71

10

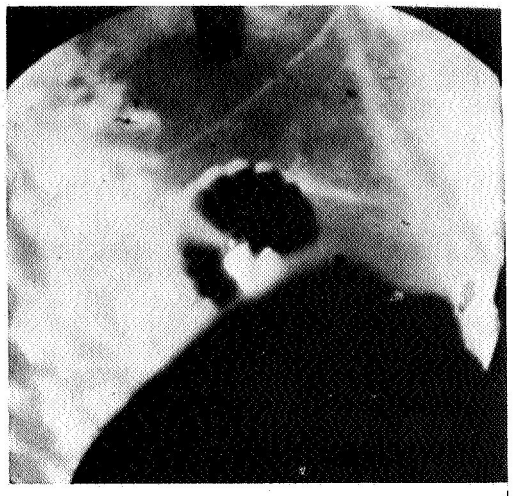

t = 61.80

11

t = 61.89

12

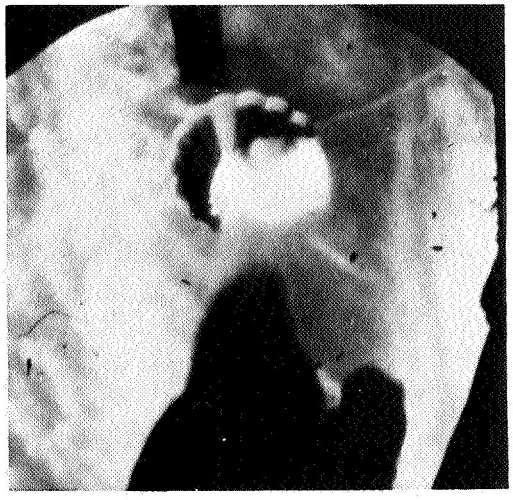

t = 61.96

Figure 11.- Continued.

L-69-5263

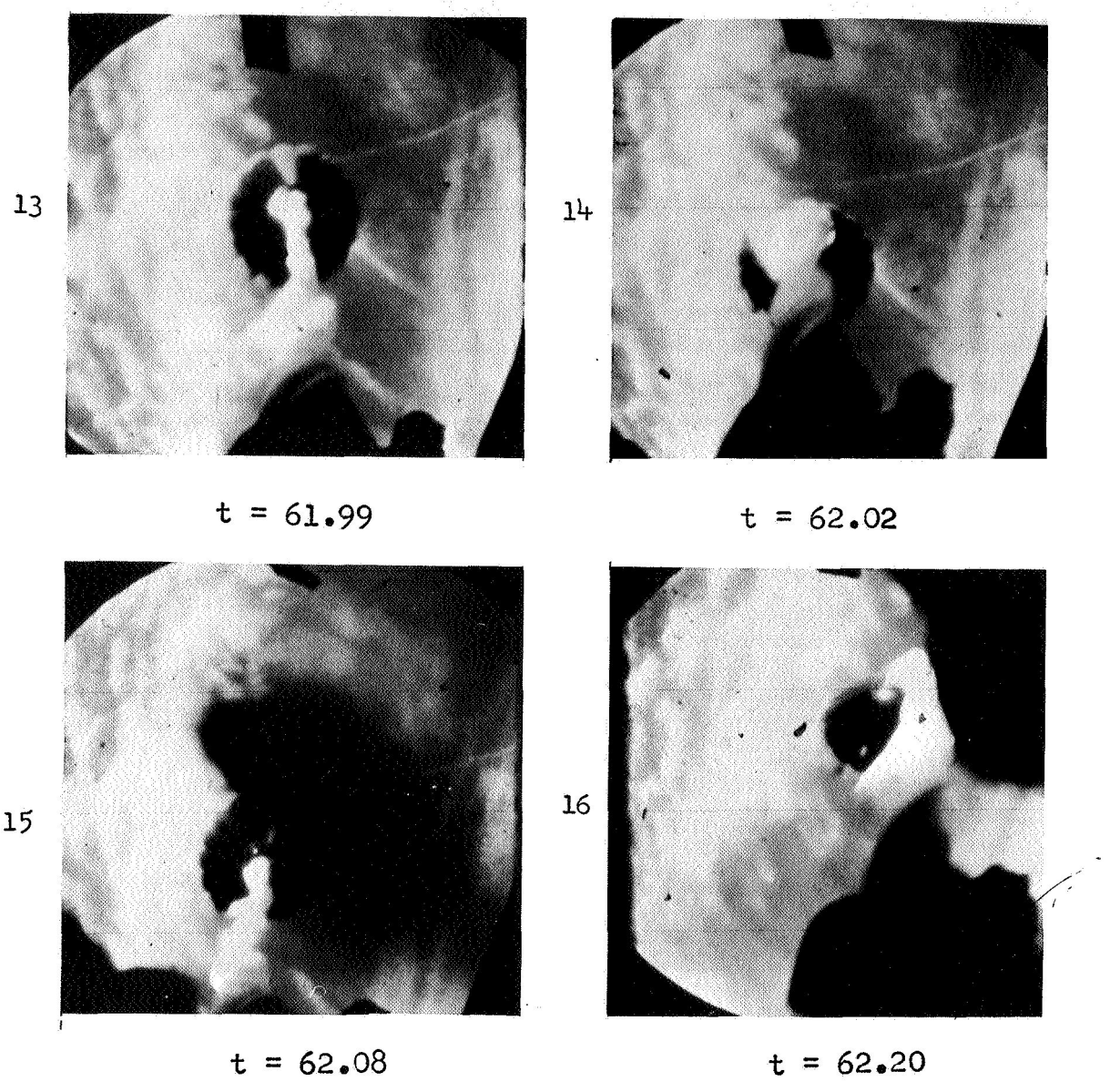

Figure 11.- Continued.

L-69-5264

17

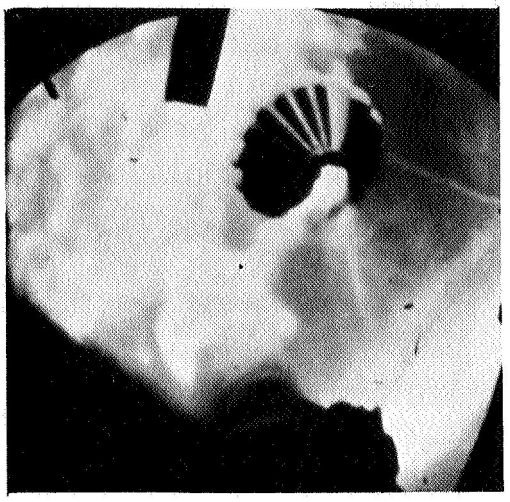

t = 62.26

18

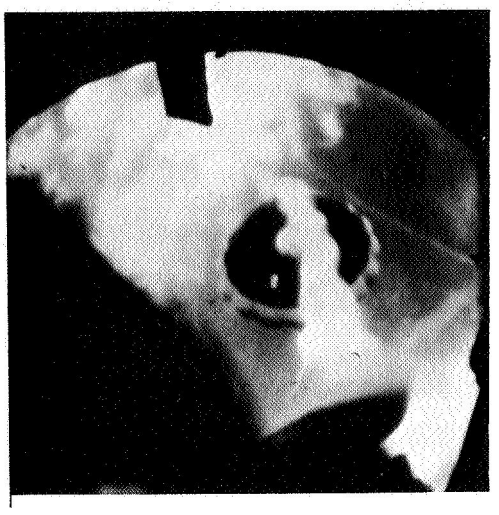

t = 62.29

19

t = 62.39

20

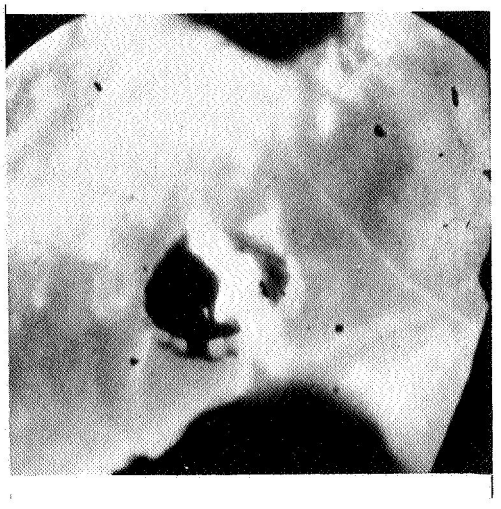

t = 62.45

Figure 11.- Continued.

L-69-5265

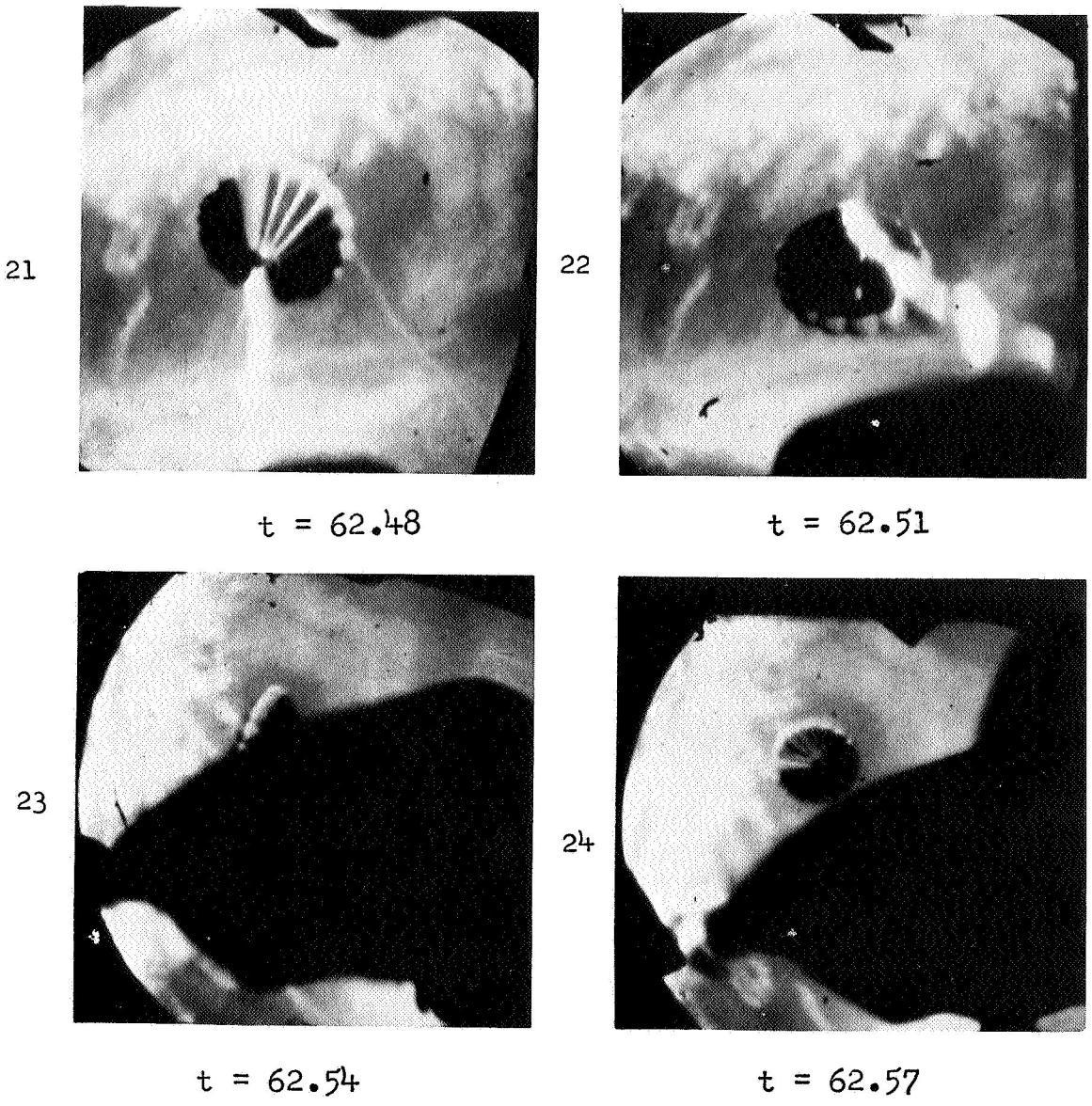

Figure 11.- Concluded.

L-69-5266

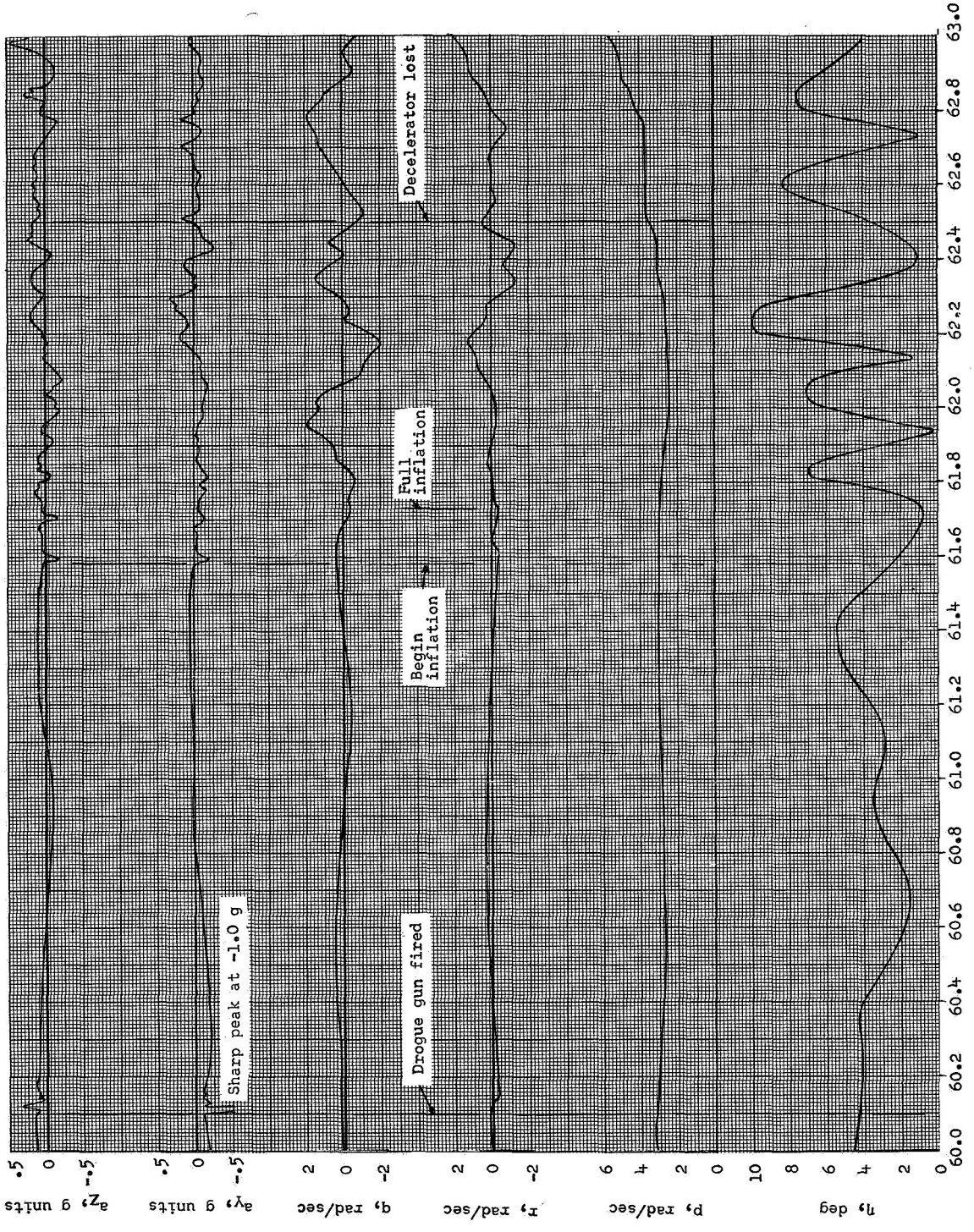

Figure 12.- Histories of a_Z, a_Y, p, q, r, and η of payload.

NASA-Langley, 1969 —— 2 L-6637

A motion-picture film supplement is available on loan. Requests will be filled in the order received. You will be notified of the approximate date scheduled.

The film (16 mm, 10 sec, color, silent) shows deployment and inflation of the decelerator and the decelerator after inflation.

Film supplement L-1049 is available on request to:

NASA Langley Research Center
Attn: Photographic Branch, Mail Stop 171
Hampton, Va. 23365

CUT

Date_____

Please send, on loan, copy of film supplement L-1049 to TM X-1833.

_____
Name of organization

_____
Street number

_____
City and State Zip code

Attention: Mr._____
Title_____

CUT

Place
Stamp
Here

NASA Langley Research Center
Attn: Photographic Branch, Mail Stop 171
Hampton, Va. 23365

1. Report No. NASA TM X-1833	2. Government Accession No.	3. Recipient's Catalog No.
4. Title and Subtitle RESULTS OF A FREE-FLIGHT TEST TO DETERMINE THE PERFORMANCE CHARACTERISTICS OF A TOWED, CONICAL DECELERATOR		5. Report Date October 1969 6. Performing Organization Code
7. Author(s) J. W. Usry		8. Performing Organization Report No. L-6637 10. Work Unit No. 124-07-03-05-23
9. Performing Organization Name and Address NASA Langley Research Center Hampton, Va. 23365		11. Contract or Grant No. 13. Type of Report and Period Covered Technical Memorandum
12. Sponsoring Agency Name and Address National Aeronautics and Space Administration Washington, D.C. 20546		14. Sponsoring Agency Code

15. Supplementary Notes

Technical Film Supplement L-1049 available on request.

16. Abstract

An inflatable fabric decelerator was tested in free flight to determine its drag and stability characteristics. The inflated decelerator approximated an 80^{0} cone with a 48-inch (121.9-cm) base and was towed behind a cone-cylinder-flare payload at a distance of 13.6 feet (4.15 m) from the payload base. The payload had a maximum flare diameter of 18.21 inches (46.25 cm). The decelerator was deployed at an altitude of 112 000 feet (34.14 km) and a velocity of 4560 ft/sec (1390 m/sec). Inflation occurred at a Mach number of 4.31 and a dynamic pressure of 130 lb/ft^2 (6224 N/m^2).

The snatch force after deployment was not more than 500 pounds (2224 N); this low force indicated that the towline assembly design could be simplified for future flights by eliminating the two snubber lines and the nylon sleeve. The shock force due to inflation was 5600 pounds (24.9 kN). After inflation the force in the towline varied between 300 and 1600 pounds (1334 and 7117 N). The oscillatory motion of the decelerator had a high frequency, and the amplitude increased with time. The test was terminated about 1 second after inflation because of a failure at the attachment point of the towline to the decelerator. The results indicated that the decelerator system was unstable and not suitable for use as a supersonic decelerator with the payload used in this experiment under the conditions of the test. A drag coefficient of 0.75 at a Mach number of 4.2 was estimated from the mean value of the force in the towline prior to the failure.

17. Key Words Suggested by Author(s)
Decelerator
Inflatable cone
Free-flight test
Towed body

18. Distribution Statement
Unclassified – Unlimited

19. Security Classif. (of this report)	20. Security Classif. (of this page)	21. No. of Pages	22. Price*
Unclassified	Unclassified	33	$3.00

*For sale by the Clearinghouse for Federal Scientific and Technical Information
Springfield, Virginia 22151

NATIONAL AERONAUTICS AND SPACE ADMINISTRATION
WASHINGTON, D.C. 20546

OFFICIAL BUSINESS

FIRST CLASS MAIL

POSTAGE AND FEES PAID
NATIONAL AERONAUTICS AN
SPACE ADMINISTRATION

POSTMASTER: If Undeliverable (Section 158
Postal Manual) Do Not Return

"The aeronautical and space activities of the United States shall be conducted so as to contribute . . . to the expansion of human knowledge of phenomena in the atmosphere and space. The Administration shall provide for the widest practicable and appropriate dissemination of information concerning its activities and the results thereof."

—NATIONAL AERONAUTICS AND SPACE ACT OF 1958

NASA SCIENTIFIC AND TECHNICAL PUBLICATIONS

TECHNICAL REPORTS: Scientific and technical information considered important, complete, and a lasting contribution to existing knowledge.

TECHNICAL NOTES: Information less broad in scope but nevertheless of importance as a contribution to existing knowledge.

TECHNICAL MEMORANDUMS: Information receiving limited distribution because of preliminary data, security classification, or other reasons.

CONTRACTOR REPORTS: Scientific and technical information generated under a NASA contract or grant and considered an important contribution to existing knowledge.

TECHNICAL TRANSLATIONS: Information published in a foreign language considered to merit NASA distribution in English.

SPECIAL PUBLICATIONS: Information derived from or of value to NASA activities. Publications include conference proceedings, monographs, data compilations, handbooks, sourcebooks, and special bibliographies.

TECHNOLOGY UTILIZATION PUBLICATIONS: Information on technology used by NASA that may be of particular interest in commercial and other non-aerospace applications. Publications include Tech Briefs, Technology Utilization Reports and Notes, and Technology Surveys.

Details on the availability of these publications may be obtained from:

SCIENTIFIC AND TECHNICAL INFORMATION DIVISION
NATIONAL AERONAUTICS AND SPACE ADMINISTRATION
Washington, D.C. 20546